

Carrier Offset and Channel Estimation for Cooperative MIMO Sensor Networks

Ronald A. Iltis, Shahnam Mirzaei and Ryan Kastner

University of California

Santa Barbara, CA 93106-9560

E-mail: iltis@ece.ucsb.edu

Richard E. Cagley and Brad T. Weals

Toyon Corporation

Goleta, CA 93117

E-mail: rcagley@toyon.com

Abstract—A cooperative MIMO network is considered with N_s sensors and a collector node with M_c antennas. In a practical implementation of this network, the sensor carriers have relative frequency offsets which must be estimated along with the MIMO channel. Generalized successive interference cancellation (GSIC) is proposed for this joint estimation problem. The primary operations in GSIC are correlation, FFT and cancellation. A reconfigurable hardware (FPGA) implementation of these GSIC primitives is described. A hybrid analysis/simulation for symbol error probability (SER) is presented with results for GSIC using Alamouti and \mathcal{G}_c^A codes.

I. INTRODUCTION

In a variety of scenarios, it is difficult or impossible for wireless sensor nodes (WSN) to achieve link connectivity due to their sparse resources including limited transmit power. While temporal coding or higher transmit power can be used to increase connectivity, these solutions are counter to the spirit of low-cost embedded wireless nodes. In addition, a WSN may only infrequently need to reach a receiver that is not co-located; it is not cost-effective to equip nodes with capabilities that will be rarely used. In this paper we provide an operational overview of our cooperative MIMO concept, discuss the GSIC algorithm for the difficult problem of joint channel/carrier/offset estimation, and address baseband implementation in reconfigurable hardware.

We consider a network with N_s single-antenna sensors and an uplink to an M_c element collector node. The concept is shown in Figure 1. It is assumed that the N_s sensors have a common pool of data \mathbf{b} to transmit, representing for example the estimated position/velocity of a jointly tracked target (labeled *Event* in the figure). Cooperative MIMO has been proposed as a method for achieving longer range and/or lower power by forming a virtual array with the sensors [1][2][3]. However, unlike point-to-point MIMO, the sensors cannot phase-lock their upconverters or symbol clocks, and thus these parameters must be jointly estimated with the MIMO channel. The GSIC algorithm [4] is a pragmatic solution to this difficult separable signal problem, and is based on successive correlation and cancellations to eliminate the exponential increase in estimator complexity using the

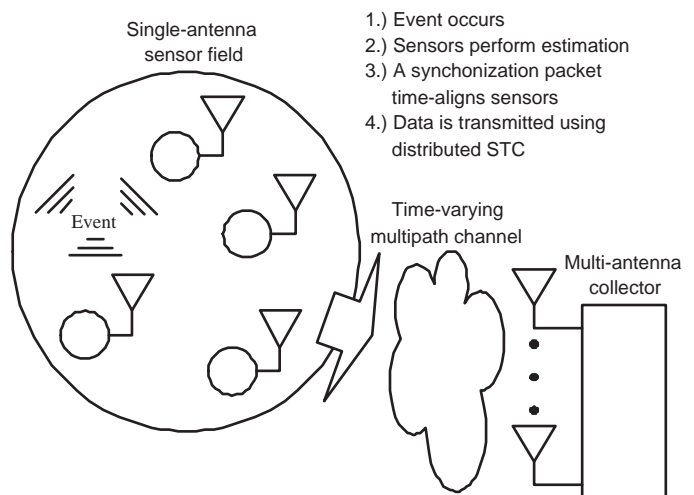


Fig. 1. Overview of operational concept.

optimal maximum-likelihood (ML) method. Specifically, each stage of GSIC corresponds to the single sensor ML solution for channel/offset/delay estimation based on cancellation of previously estimated sensor received waveforms.

In order to rapidly evaluate GSIC performance, a hybrid analysis/simulation method for SER evaluation is presented based on union bound and nearest-neighbor (NN) error rate approximations. It is shown that the orthogonal columns in an OSTBC [5] lead to a distance-preservation property for error sequences and thus a simple computation of the NN error rate.

In the hardware development section of the paper we discuss RF and baseband design issues. Our primary focus for RF design is to achieve stability of the voltage-controlled oscillators (VCOs). A secondary consideration is high sensitivity to a large sum of individually low-power sensor signals. We show resource use for two candidate field programmable gate arrays (FPGA), namely Xilinx Spartan-3 and Virtex-4 devices. While many design features, such as channel tracking and decoding, are identical to those in conventional MIMO designs with co-

located antenna elements, there are special considerations that must be made for parameter estimation in the cooperative sensor problem. Since the individual sensor oscillators are not co-located, they cannot be phase-locked, and hence the received sensor offsets must be estimated individually at the collector. This design issue represents the core reason for the necessity of GSIC.

In the sequel, the cooperative MIMO channel is defined in Section II along with the GSIC algorithm for offset/channel estimation. The NN error bound is developed in Section IV and the reconfigurable hardware design is summarized in Section V. The results of the hybrid analysis/simulation are given in Section VI along with conclusions.

II. COOPERATIVE MIMO CHANNEL AND ESTIMATION PROBLEM

A flat-fading channel is assumed between the N_s sensors and collector with M_c elements. The received collector signal $\mathbf{r}_c(t) \in \mathbb{C}^{M_c}$ on the uplink is then given in continuous-time by

$$\mathbf{r}_c(t) = \sum_{k=1}^{N_s} \mathbf{h}_k \sum_{m=0}^{\infty} p(t - \tau_k - mT) e^{i\delta\omega_k t} s_k(m) + \mathbf{n}(t), \quad (1)$$

where $\mathbf{h}_k \in \mathbb{C}^{M_c}$ is the flat-fading channel from sensor k to the collector, ω_k is the frequency offset in Hz for sensor k , and τ_k is the corresponding delay. The symbols $s_k(m) \in \mathbb{C}$ represent a training sequence in the estimation phase, or the m -th row and k -th column of an OSTBC matrix [5]. The symbols are normalized to $E\{|s_k(m)|^2\} = 1$. The pulses $p(t)$ are raised-cosine with minimal excess bandwidth to maximize orthogonality. The bandpass pulse energy *per sensor* is defined by $E_s = \int p(t)^2 dt$, so that the total transmitted bandpass energy is $E_s N_s$ per information symbol for OSTBCs. Note that this is in contrast to the conventional MIMO normalization but represents the more realistic case of fixed sensor transmit power.

A discrete-time signal model is obtained by defining the matrix of samples collected from the M_c elements, $\mathbf{R}(m) \in \mathbb{C}^{N_c \times M_c}$ as

$$\mathbf{R}(m) = \sum_{k=1}^{N_s} \sum_{q=0}^{N_c-1} \mathbf{p}_{q,m}(\tau_k, \delta\omega_k) \mathbf{h}_k^T s_k(q + mN_c) + \mathbf{N}(m). \quad (2)$$

In (2), N_c corresponds to the number of symbols/training packet, or temporal length of the OSTBC, with m denoting the packet or OSTBC symbol index. The elements of $\mathbf{N}(m)$ are i.i.d. circular Gaussian with variance $2N_0/T_s$, assuming an input Nyquist bandwidth $1/(2T_s)$. The pulse vectors $\mathbf{p}_{q,m} \in \mathbb{C}^{N_c N_d}$ are defined by

$$\begin{aligned} \mathbf{p}_{q,m}(\tau_k, \delta\omega_k) = & \quad (3) \\ & \left[p((N_c N_d - 1)T_s - \tau_k - qT) e^{i\delta\omega_k(mN_c T + (N_c N_d - 1)T_s)}, \right. \\ & \left. \dots, p(-\tau_k - qT) e^{i\delta\omega_k m N_c T} \right]^T, \end{aligned}$$

where $1/T$ is the symbol rate and $N_d = T/T_s$ is the oversampling factor. Note our reconfigurable hardware solution uses $N_d = 32$ for precision delay τ_k estimation.

Let $m = 0$ w.l.o.g. in (3). The joint estimation problem then becomes

$$\begin{aligned} \{\hat{\tau}_k, \hat{\mathbf{h}}_k, \hat{\delta\omega}_k\} = \arg \min_{\{\tau_k, \mathbf{h}_k, \delta\omega_k\}} & \quad (4) \\ \|\mathbf{R} - \sum_{k=1}^{N_s} \sum_{q=0}^{N_c-1} \mathbf{p}_q(\tau_k, \delta\omega_k) \mathbf{h}_k^T s_k(q)\|_F^2. & \end{aligned}$$

where $\|\mathbf{X}\|_F$ is the Frobenius norm. The focus here is on known training symbols $s_k(q)$. Although blind MIMO channel/offset estimators have been developed [6], the required eigendecompositions are too complex for the reconfigurable hardware available here. Thus we assume Gold-sequence training packets $\{s_k(q)\}$ for estimation in eq. (4).

III. CORRELATION AND GSIC ESTIMATION ALGORITHMS

When the node symbol clocks are synchronized such that $\tau_k = \tau$ for all k , and orthogonal training sequences $\{s_k(q)\}$ are employed, the estimation problem (4) becomes separable in nodes k . However, when relative timing offsets are present, multiuser interference between sensor waveforms necessitates exponentially complex in N_s joint optimization to obtain the maximum-likelihood solution.

To obtain a practical algorithm in reconfigurable hardware, we propose to approximate (4) using the Generalized Successive Interference Cancellation approach in [4]. Note that stage 1 of GSIC corresponds to N_s independent correlations and is thus optimal for synchronized nodes and orthogonal sequences. Thus we can balance levels of cancellation and hardware complexity to obtain a feasible collector estimation algorithm. At iteration k of GSIC, a cancelled signal matrix \mathbf{R}^k is available. The ML joint estimates of $\delta\omega_l, \tau_l, \mathbf{h}_l$ are then computed for $l \in \{1, \dots, N_s\} \setminus \{p_1, \dots, p_{k-1}\}$, where p_k is the sensor index selected on GSIC iteration k . The index p_k is chosen from the joint estimates $\hat{\delta\omega}_l, \hat{\tau}_l, \hat{\mathbf{h}}_l$ that best fit the residual \mathbf{R}^k . The residual \mathbf{R}^{k+1} is then updated using the cancellation

$$\mathbf{R}^{k+1} = \mathbf{R}^k - \sum_{q=0}^{N_c-1} \mathbf{p}_q(\hat{\tau}_{p_k}, \hat{\delta\omega}_{p_k}) \hat{\mathbf{h}}_{p_k}^T s_{p_k}(q). \quad (5)$$

The key step in GSIC is finding the intermediate estimates in indices l . These are defined at iteration k by

$$\hat{\tau}_l, \hat{\delta\omega}_l, \hat{\mathbf{h}}_l = \arg \min_{\tau_l, \delta\omega_l, \mathbf{h}_l} \|\mathbf{R}^k - \sum_{q=0}^{N_c-1} \mathbf{p}_q(\tau_l, \delta\omega_l) \mathbf{h}_l^T s_l(q)\|_F^2. \quad (6)$$

The channel estimate $\hat{\mathbf{h}}_l$ conditioned on $\tau_l, \delta\omega_l$ is readily shown to equal

$$\hat{\mathbf{h}}_l = \frac{1}{\sum_{q=0}^{N_c-1} \|\mathbf{p}_q(\tau_l, \delta\omega_l)\|_F^2 |s_l(q)|^2} \sum_{q=0}^{N_c-1} (\mathbf{R}^k)^T \mathbf{p}_q(\tau_l, \delta\omega_l)^* s_l(q)^*. \quad (7)$$

Initialize $\mathbf{R}^1 = \mathbf{R}(m)$
For $k = 1, 2, \dots, N_s$
For $l = 1, \dots, N_s \setminus \{p_1, \dots, p_{k-1}\}$
$\hat{\tau}_k, \hat{\delta\omega}_l = \arg \max_{\tau_l, \delta\omega_l} \gamma_l(\tau_l, \delta\omega_l)$ where
$\gamma_l(\tau_l, \delta\omega_k) = \frac{\left\ \sum_{q=0}^{N_c-1} (\mathbf{R}^k)^T \mathbf{p}_q^*(\tau_l, \delta\omega_l) s_l(m')^* \right\ ^2}{\sum_{q=0}^{N_c-1} \ \mathbf{p}_q(\tau_l, \delta\omega_l)\ ^2 s_l(q) ^2}$
Next l
$p_k = \arg \max_l \gamma(\hat{\tau}_l, \hat{\delta\omega}_l)$
$\hat{\mathbf{h}}_{p_k} = \frac{\sum_{q=0}^{N_c-1} (\mathbf{R}^k)^T \mathbf{p}_q(\hat{\tau}_{p_k}, \hat{\delta\omega}_{p_k})^* s_{p_k}(q)^*}{\sum_{q=0}^{N_c-1} \ \mathbf{p}_q(\hat{\tau}_{p_k}, \hat{\delta\omega}_{p_k})\ ^2 s_{p_k}(q) ^2}$
$\mathbf{R}^{k+1} = \mathbf{R}^k - \sum_{q=0}^{N_c-1} \mathbf{p}_q(\hat{\tau}_{p_k}, \hat{\delta\omega}_{p_k}) \hat{\mathbf{h}}_{p_k}^T s_{p_k}(q)$
Next k

TABLE I

GSIC ALGORITHM FOR JOINT CHANNEL/DELAY/OFFSET ESTIMATION – TRAINING

It is assumed that the raised-cosine pulse vectors are approximately orthogonal for minimal excess bandwidth. That is $\mathbf{p}_q(\tau_l, \delta\omega_l)^H \mathbf{p}_{q'}(\tau_l, \delta\omega_l) \approx \frac{2E_s}{T_s} \delta_{q,q'}$. Inserting the conditional estimate from (7) and employing the pulse vector orthogonality in (6) gives the estimates for delay and offset.

$$\hat{\tau}_l, \hat{\delta\omega}_l = \arg \max_{\tau_l, \delta\omega_l} \frac{\left\| \sum_{q=0}^{N_c-1} (\mathbf{R}^k)^T \mathbf{p}_q^*(\tau_l, \delta\omega_l) s_l(q)^* \right\|^2}{\sum_{q=0}^{N_c-1} \|\mathbf{p}_q(\tau_l, \delta\omega_l)\|^2 |s_l(q)|^2}. \quad (8)$$

The GSIC algorithm for training symbols is summarized in Table I.

IV. HYBRID ANALYSIS/SIMULATION OF COOPERATIVE MIMO SER

The symbol error rate analysis for MIMO systems is usually based on averaging bounds for pairwise error probability (PEP) w.r.t. circular Gaussian statistics for the channel $\{\mathbf{h}_k\}$ [7][8]. However, the channel/offset estimation errors in GSIC are difficult to characterize analytically, and thus we pursue a hybrid analysis/simulation approach. That is, an analytic bound for SER P_e is obtained conditioned on simulated values of $\{\tau_k, \delta\omega_k, \mathbf{h}_k\}$ and their corresponding estimates, thus obtaining a closed-form solution for $P_e(n)$ at each simulation iteration. Time-averaging of $P_e(n)$ leads to an estimate of unconditional SER, assuming ergodicity of the channel/offsets and estimation errors.

To minimize simulation time, we employ a nearest-neighbor approximation to the error rate union bound as follows. First consider the PEP for known channels, which can be shown to equal

$$P_2^{n,n'} = \frac{1}{2} \operatorname{erfc} \left(\frac{\|\mathbf{S}^n - \mathbf{S}^{n'}\|_F}{\sqrt{\frac{8N_0}{T_s}}} \right), \quad (9)$$

where \mathbf{S}^n is the noiseless received space-time signal. Specifically, $\mathbf{R} = \mathbf{S}^n + \mathbf{N}$ for the n -th OSTBC codeword, and

$$\mathbf{S}^n = \sum_{k=1}^{N_s} \sum_{q=0}^{N_c-1} \mathbf{p}_q(\tau_k, \delta\omega_k) \mathbf{h}_k^T s_k^n(q) \quad (10)$$

For OSTBCs, N_s symbols $b_1^n \dots b_{N_s}^n \in \mathbb{C}\mathbb{Z}$ are mapped to the $N_c \times N_s$ matrix with components $s_k^n(q)$ following [5]. A union bound for SER can be computed by summing $P_2^{n,n'}$ (9) over all codewords $n' \neq n$. However, M-ary QAM requires summing over $M^{N_s} - 1$ such terms.

The following proposition is readily proved using the orthogonality of the columns of the OSTBC and orthogonality of the pulse vectors \mathbf{p}_q .

Proposition 1: Let the Euclidean distance between information sequences equal $d_{n,n'} = \sum_{l=1}^{N_s} |b_l^n - b_l^{n'}|^2$. Then the Frobenius error norm between the space-time received matrices satisfies

$$\|\mathbf{S}_m^n - \mathbf{S}_m^{n'}\|_F^2 = \frac{8E_s}{T_s} d_{n,n'} \sum_{k=1}^{N_s} \|\mathbf{h}_k\|^2 \quad (11)$$

The significance of Proposition 1 is that the minimum PEP corresponds to the information sequences with minimum Euclidean distance – this is a direct consequence of the pulse function orthogonality and properties of orthogonal designs.

For QPSK, $d_{min} = 1$ for normalization $|b_l^n|^2 = 1$. The NN approximation to the union bound yields

$$P_e \approx \frac{2N_s}{2} \operatorname{erfc} \left(\sqrt{\frac{E_s \sum_{k=1}^{N_s} \|\mathbf{h}_k\|^2}{N_0}} \right), \quad (12)$$

where it is noted that there are $2N_s$ possible near-neighbor error events n, n' for QPSK. The PEP conditioned on estimation errors for simulation iteration m is

$$P_2(n, n') = P \left(\|\mathbf{R}(m) - \hat{\mathbf{S}}_m^n\|_F^2 > \|\mathbf{R}(m) - \hat{\mathbf{S}}_m^{n'}\|_F^2 \right), \quad (13)$$

where $\hat{\mathbf{S}}_m^n(m)$ corresponds to (10) with quantities $\tau_k, \delta\omega_k, \mathbf{h}_k$ replaced by their respective GSIC estimates. Considering only those n' corresponding to NN error events yields the conditional SER approximation at iteration m

$$P_e(m) \approx \frac{2N_s}{2} \operatorname{erfc} \left(\frac{\|\mathbf{S}_m^n - \hat{\mathbf{S}}_m^{n'}\|_F - \|\mathbf{S}_m^n - \hat{\mathbf{S}}_m^n\|_F}{\sqrt{\frac{8N_0}{T_s} \|\hat{\mathbf{S}}_m^n - \hat{\mathbf{S}}_m^{n'}\|_F^2}} \right). \quad (14)$$

Time-averaging of $P_e(m)$ yields the hybrid analysis/simulation of SER.

V. HARDWARE DESIGN

Applying an OSTBC to a distributed array of sensors represents a significant advancement in complexity in terms of the communications protocol and link setup. Naturally, the hardware design must be able to provide the needed feature set in order to implement such an architecture. The two principle considerations are timing and frequency offsets.

Obviously, if there is poor time synchronization then the sensor OSTBC signals will not be time-aligned at the collector,

resulting in a loss of orthogonality and the introduction of inter-symbol interference (ISI). The timing problem is dealt with by using a high oversampling rate for good delay resolution, and downlink timing control. The GSIC-derived delay estimates are then used to calculate the appropriate sensor symbol clock corrections. Alternatively, a common synchronization beacon can be used; this can be sent by either the collector or a local sensor node. In either case, oversampling rates of $N_d \geq 16$ are needed in order to maintain timing synchronization. Alternative techniques, such as the use of the global positioning system (GPS), have been explored but lack the fidelity for the target rates of our hardware.

The complexity of the joint frequency-offset estimation problem is driven by the absolute maximum offset between the sensor node and collector, level of fidelity, and number of sensor nodes. Driving the overall design is the maximum frequency offset level for which we must compensate. Our RF design offers a production capable 0.5 parts per million (PPM) maximum offset at the carrier frequency with a maximum of 4.5 PPM after ten years of operation. Thus, while we will typically encounter offsets that are a maximum of 1 kHz, we must be able to provide compensation for up to 10 kHz over the life of the equipment. These considerations, and the required fidelity of the tolerable frequency offset in channel tracking, drive the required search range of our frequency offset estimation.

The overall architecture of the collector demodulation is shown in Figure 2. In terms of the GSIC algorithm, our primary area of consideration is the timing and frequency estimation block. The collector antennas are co-located and hence have high correlation in their receive channel statistics. Furthermore, the separate collector RF sections are driven by a single VCO meaning the relative offsets at each collector antenna are the same. In Table II we show the relative resource use and power consumption for the different portions of our FPGA baseband processing design. The most expensive portion of the design is the single-stage GSIC (correlation method without cancellation), which provides timing and frequency offset estimates. This process involves a sample-by-sample multiplication with the training sequence and then an FFT. The output of the FFT provides an indication of the degree to which the received signal is correlated with the training sequence (indicating timing) as well as the frequency (indicating offset).

The primary operation in GSIC is the correlation/FFT operation. From Table I, the columnwise correlations of \mathbf{R} can be written as (Matlab notation)

$$\begin{aligned} \mathbf{R}(:, i)^T \mathbf{p}_q^*(\tau_l, \delta\omega_l) \\ = \sum_{m=0}^{N_c N_d - 1} \mathbf{R}(m, i) s_l(mT_s - \tau_l) e^{-i2\pi\delta\omega_l mT_s}, \end{aligned} \quad (15)$$

where $s_l(mT_s - \tau_l) = \sum_{q=0}^{N_c - 1} s_l(q)p(mT_s - qT - \tau_l)$ is the effective training sequence modulated by the pulse function. By quantizing $\delta\omega_l$ to the integer FFT frequencies and zero padding if necessary, (15) is (a) the Hadamard product of the received samples per antenna with the training sequence

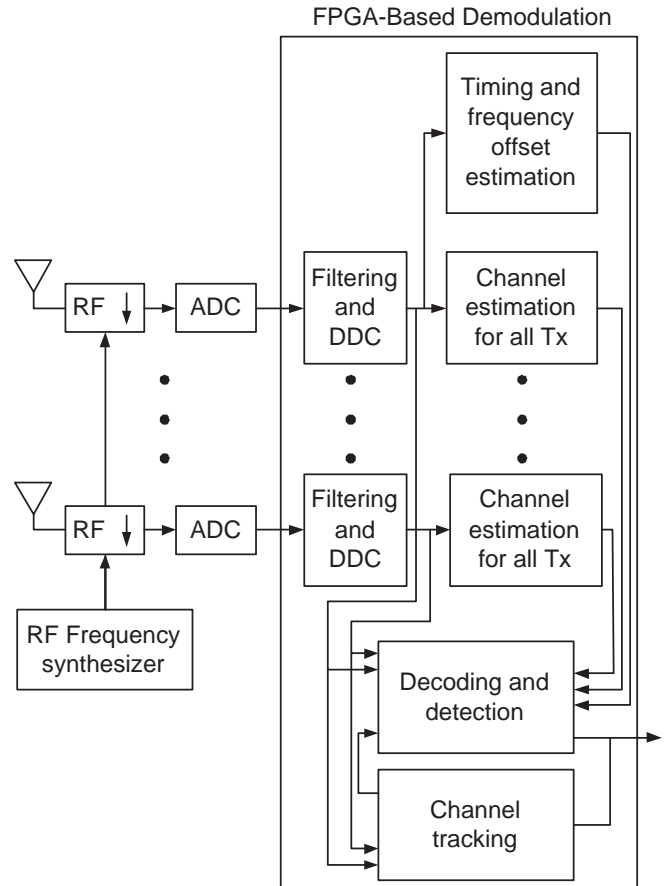


Fig. 2. Collector demodulation architecture.

$s_l(mT_s)$ followed by an FFT which simultaneously performs the required correlation. We note that the throughput of the overall design is constrained by the FFT operation as it must operate at the oversampled rate, whereas all other portions of the design operate at the symbol rate. There is a trade-off in terms of latency (throughput) versus resource use in the FFT. That is, if higher degrees of parallelism are used then there is a throughput increase, with the corresponding requirement of additional hardware resources.

VI. RESULTS AND CONCLUSIONS

The analysis/simulation error rate approximation (14) was computed for cases of (a) $N_s = 2$ sensors using the Alamouti code and (b) $N_s = 4$ sensors using \mathcal{G}_c^4 in [5]. A collector with $M_c = 4$ antennas was used for both codes. In addition to GSIC estimation, a correlation method was also employed. Correlation corresponds to the first GSIC iteration only and thus excludes subsequent cancellation steps. At each simulation iteration, a channel/offset estimate was computed based on $N_c = 63$ length quasi-orthogonal Gold sequences transmitted by each sensor. The SER approximation (14) was then computed based on these estimates.

Fig. 3 shows the analysis/simulation SER estimates. The \mathcal{G}_c^4 4x4 code performance is 4.5 dB better than Alamouti 2x4

	XC3S2000-5FG676						XC4VSX35-12FF668							
	Area					Rate (ns)	Power (mW)	Area					Rate (ns)	Power (mW)
	FF	LUT	SLICE	BRAM	Mult.			FF	LUT	SLICE	BRAM	DSP		
Available Resources	40960	40960	20480	40	40	N/A	N/A	30720	30720	15360	192	192	N/A	N/A
Transceiver (Top Level)	17507	14143	11184	14	22	16.61		17187	13745	10673	14	22	8.89	
DDC	1247	892	750	0	0	10.42		1247	892	750	0	0	4.95	
One-Stage GSIC	9649	5795	7047	12	12	18.66		9239	5531	6745	12	12	10.18	
Channel Tracking	2313	2201	1397	0	0	10.43		2313	2201	1397	0	0	6.7	
DUC	2475	1207	1401	2	10	11.57		2190	1206	1258	2	10	5.54	

TABLE II
RESOURCE USE AND POWER CONSUMPTION FOR SPARTAN-3 AND VIRTEX-4 FPGAS.

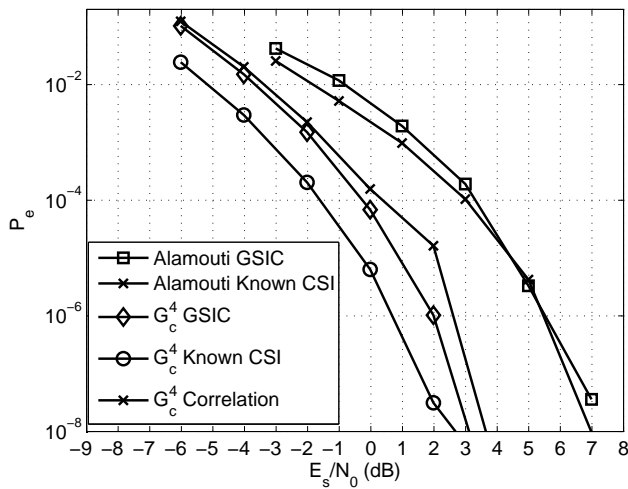


Fig. 3. Nearest-neighbor/union bound SER results for GSIC and Correlation.

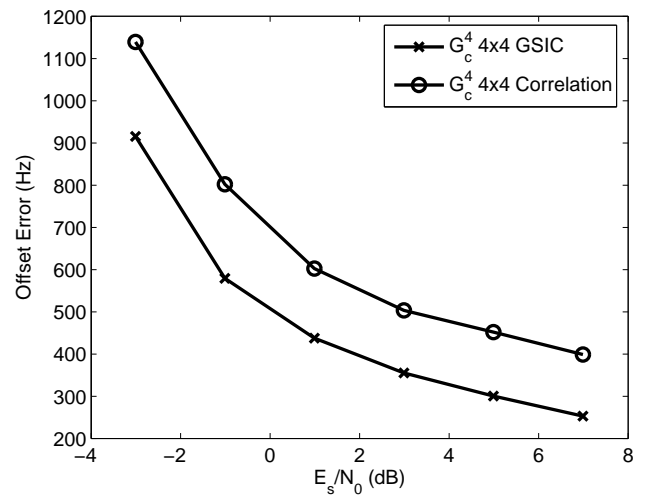


Fig. 4. Frequency offset estimation errors using GSIC vs. Correlation.

at 10^{-4} SER. This performance gain is due to (a) increased transmit diversity gain of G_c^4 , and (b) A 3 dB increase in E_s for the 4×4 code over the Alamouti code (2×2), since the individual sensor transmit power is the same for both schemes. The frequency offset estimation error is shown in Fig. 4 for G_c^4 using the GSIC and correlation methods. As expected, the cancellation in GSIC yields lower offset errors of almost 200 Hz.

To conclude, GSIC appears to be a practical solution to the joint channel/offset/delay estimation problem in cooperative MIMO sensor networks. Improvements to the GSIC approach yielding higher computational efficiency, and further optimization of codes and training sequences should be investigated.

ACKNOWLEDGMENT

This work was supported by the Air Force Office of Scientific Research under Contract No. FA9550-05-C-0179 and Toyon Research Corporation Subcontract No. SC-06-5477-1

REFERENCES

[1] J. N. Laneman and G. W. Wornell, "Distributed space-time-coded protocols for exploiting cooperative diversity in wireless networks," *IEEE Transactions on Information Theory*, vol. 49, pp. 2415–2425, Oct. 2003.

[2] S. J. Kim, R. E. Cagley, and R. A. Iltis, "Spectrally efficient communication for wireless sensor networks using a cooperative MIMO technique," *Wireless Networks*, (To Appear).

[3] S. Cui, A. Goldsmith, and A. Bahai, "Energy efficiency of MIMO and cooperative MIMO techniques in sensor networks," *IEEE Journal on Selected Areas in Communications*, vol. 22, pp. 1089–1098, Aug. 2004.

[4] R. Iltis and S. Kim, "Geometric derivation of Expectation-Maximization and Generalized Successive Interference Cancellation algorithms with applications to CDMA channel estimation," *IEEE Transactions on Signal Processing*, vol. 51, pp. 1367–1377, May 2003.

[5] V. Tarokh, H. Jafarkhani, and A. Calderbank, "Space-time block coding for wireless communications: Performance results," *IEEE Journal on Selected Areas in Communications*, vol. 17, pp. 451–460, March 1999.

[6] S. Shahbazpanahi, A. Gershman, and J. Manton, "Closed-form blind MIMO channel estimation for orthogonal space-time block codes," *IEEE Transactions on Signal Processing*, vol. 53, pp. 4506–4517, 2005.

[7] V. Tarokh, N. Seshadri, and A. Calderbank, "Space-time codes for high data rate wireless communications: Performance criterion and code construction," *IEEE Transactions on Information Theory*, pp. 744–765, March 1998.

[8] M. Brehler and M. K. Varanasi, "Asymptotic error probability analysis of quadratic receivers in Rayleigh-fading channels with application to a unified analysis of coherent and noncoherent space-time receivers," *IEEE Transactions on Information Theory*, vol. 47, pp. 2383–2399, Sept. 2001.